CHAPTER TWO HUNDRED SEVEN

Mathematical Modelling of Water-quality for long time periods

P Huizinga*

ABSTRACT

This paper presents a one-dimensional dynamic water-quality model suitable for long-term application to estuaries. The computation techniques used in the model are very simple, but very good results have been obtained both for theoretical test cases and from applications to estuaries when compared with prototype measurements.

1. INTRODUCTION

To investigate water-quality problems in several narrow tidal estuaries in South Africa a mathematical model was required which could be applied easily and economically for long-period investigations. The model presented in this paper has certain features similar to that described by Orlob (1972) and in applying the model in combination with a one-dimensional explicit hydrodynamic model, very good results were obtained.

A brief description is given of the method employed. Some test results are shown of simulations in theoretical channels. The paper includes calibration and verification results of an application to the Knysna estuary, which is located 500 km east of Cape Town on the south coast of South Africa, as well as results of investigations of the effect of changes in fresh-water inflow on the salinity distributions in this estuary.

2. THE COMPUTATIONAL METHOD

2.1 General

One-dimensional advection and dispersion is described by the formula (see list of symbols):

$$\frac{\partial(Vol.C)}{\partial t} = \frac{\partial(Ax.K.\frac{\partial C}{\partial x})}{\partial x}.dx - \frac{\partial(Ax.uC)}{\partial x}.dx \qquad (2\text{-}1)$$

Extra terms can be included for other phenomena such as breakdown and growth or lateral inflows of contaminants.

Computational schemes are often designed for a simplified version of this equation in which constant velocity, depth and cross-sectional area are assumed:

* National Research Institute for Oceanology, Stellenbosch, Republic of South Africa.

$$\frac{\partial C}{\partial t} + u\frac{\partial C}{\partial x} = K\frac{\partial^2 C}{\partial x^2} \qquad (2\text{-}2)$$

Mathematical models based on this formula can give very good results if applied to channels and rivers with almost constant flow and cross-sectional area. They should not be applied to estuaries with complex topography and under tidal influence.

The computational method on which this model is based is similar in certain respects to that described by Orlob (1972). In principle it is based on a finite difference approximation of the equation 2-1. It consists of two stages per timestep, first, the total advective and diffusive transport between nodes are computed, in other words the right-hand side of formula 2-1 is computed. Then, knowing the change in volume in a node and also the in- and outflow volumes and concentrations, the new concentration for each node can be computed. Special routines are used to handle side branches with splitting points and positions where pollutants are released.

2.2 Advective Transport Computation

The advective transport through a cross-section during a time-step can be computed directly from the flow through that cross-section for that timestep multiplied by the average concentration. For section M-1 or between nodes N-1 and N on Figure 1 this transport is:

$$ATR_{M-1} = Q_{M-1}.C_{M-1}.\Delta t \qquad (2\text{-}3)$$

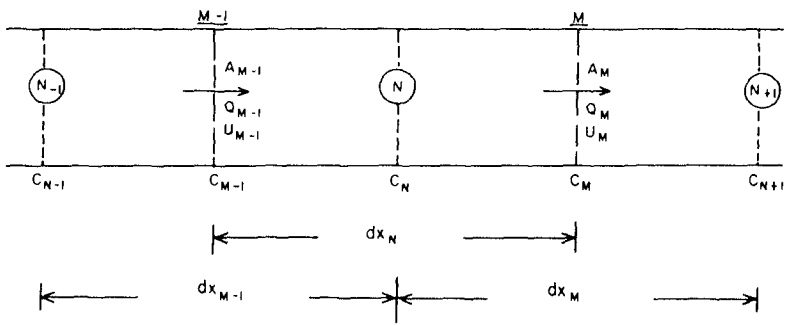

Figure 1.

Similarly for section M:

$$ATR_M = Q_M.C_M.\Delta t \qquad (2\text{-}4)$$

If there are no side branches at nodes N-1, N or N+1 a linear interpolation together with a slight correction due to the velocity U can be made to determine C_M:

$$C_M = C_N + (C_{N+1} - C_N).(0,5.dx_M - 0,5.U_N.\Delta t)/dx_M \quad (2\text{-}5)$$

and

$$C_{M-1} = C_{N-1} + (C_N - C_{N-1}).(0,5.dx_{M-1} - 0,5.U_{M-1}.\Delta t)/dx_{M-1} \quad (2\text{-}6)$$

At release positions and at splitting points sudden changes of concentrations can occur. For those situations other interpolation routines are used to estimate concentrations through cross-sections (C_M). If C_{N+1} is a splitting point and C_N not, then C_M is determined by linear extrapolation from C_{N-1} and C_N. If this would cause negative values for C_M, then C_M is set equal to zero. If C_N and C_{N+1} are splitting points and the flow is to the right then C_M is taken to be equal to C_N.

2.3 Dispersive Transport Computation (Figure 1)

Dispersion in estuaries has been extensively described by many authors (see for example, Fisher, 1979), but no predictive formula exists that can be generally applied to determine the dispersion coefficient (K) For a number of tests described in this report the coefficient was determined as suggested by Leendertse (1970). This consists of a constant part and a part dependent on velocity, depth and Chezy-coefficient.

$$K = \frac{Df/U/.R}{Cf} + Dw \quad (2\text{-}7)$$

In the salinity tests for the Knysna estuary the dispersion coefficient was determined from the salinity distribution in the estuary and the inflow of fresh water.

$$K = \frac{(\partial S/\partial x)}{(\overline{U_n}).S} \quad (2\text{-}8)$$

U_n is the net downstream velocity caused by the freshwater discharge.

The dispersive transport through a cross-section (Figure 1) during a timestep (Δt) is computed by:

$$DTR_{M-1} = -K_{M-1}.(C_N - C_{N-1}).\Delta t.A_{M-1}/dx_{M-1} \quad (2\text{-}9)$$

and

$$DTR_M = K_M\,(C_{N+1} - C_N).\Delta t.A_M/dx_M \quad (2\text{-}10)$$

2.4 Computation of Concentrations

After having computed the transports through all the cross-sections and also knowing the changes in volumes for all the nodes, the next step is to compute the new concentrations at all the nodal points. CTR_N, the total transport through all the sections leading to nodal point N, is then used to compute the new concentration at node N.

$$C^1_N = (C_N.Vol_N + CTR_N)/Vol^1_N \qquad (2\text{-}11)$$

If N is also an outfall release position, the extra transport towards N due to this outflow is also included in CTR_N.

2.5 Stability and Accuracy

The water quality model is connected to an explicit one-dimensional hydrodynamic model (CSIR, 1976) and is operated at the same schematization and timestep. This set-up implies certain disadvantages but model simulations have shown that it is a practical combination.

For stability reasons the timestep of the hydrodynamic computation is limited due to the Courant criterion.

$$\Delta t < \frac{\Delta x}{\sqrt{gR}} \qquad (2\text{-}12)$$

For advective transport only a similar criterion is valid for the water quality computation.

$$\Delta t < \frac{\Delta x}{u} \qquad (2\text{-}13)$$

The celerity of the long wave ($\sqrt{gR}$) is normally an order of magnitude faster than the water velocity. Therefore, if both models are operated on the same timestep, the Courant criterion for the hydrodynamic model determines the timestep of the computation.

Normally the water level variation with time and distance is gradual, but, variations of concentrations can be sudden which means that the section lengths in the water quality model must be small.

Therefore, in this model combination, the section length is selected first, based on the topography and on the accuracy wanted from the water quality computation, and then the timestep is set, based on the Courant criterion for the hydrodynamic computation.

2.6 Adaptation to Topography

The model has facilities to adapt cross-sectional areas, hydraulic radii, surface areas and volumes for increasing and decreasing of water levels, which makes it particularly suitable for applications to tidal estuaries.

3. RESULTS IN THEORETICAL CHANNELS

3.1 General

A few model tests were done for theoretical channels with rectangular cross-sections to test the quality of the computation techniques.

3.2 Channel with Rectangular Cross-section

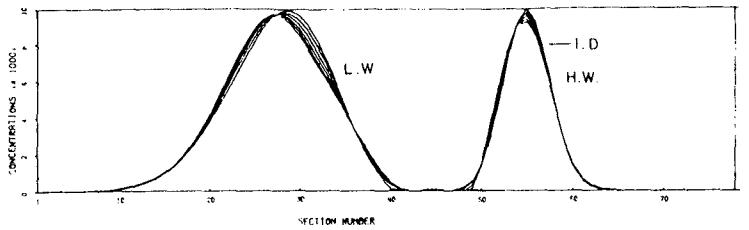

Figure 2.

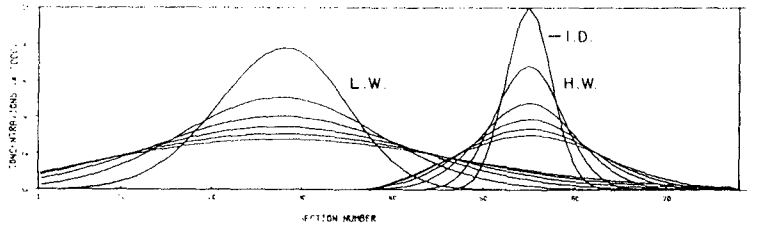

Figure 3.

The results of tests on numerical dispersion in a straight channel are shown in Figures 2 and 3. The channel has a depth of 2 m and a length of 15 400 m. It is open on the left-hand side where a water level variation with an amplitude of 1 m and a period of 12,5 hours was applied, and it is closed off on the right-hand side. The initial distribution of a conservative pollutant is indicated by I.D. and the computed concentrations at high and low water are marked by H.W. and L.W. The graphs at high and low water are plotted at intervals of 25 hours. In the first test (Figure 2) only advective transport was taken into account and in the second test (Figure 3) dispersive transport was computed as well, with a dispersion coefficient of 6,0 m^2/s. The very small deformation of the graphs on Figure 2 shows that the numerical dispersion is very small compared to the dispersion in the second test (Figure 3).

3.3 Channel with Branching

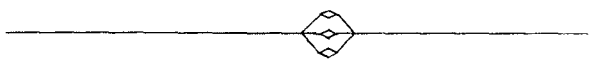

Figure 4.

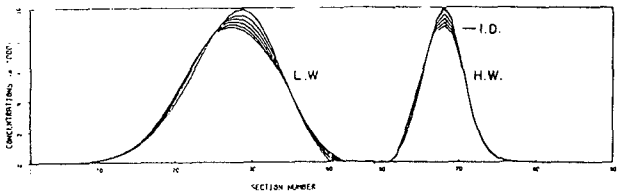

Figure 5.

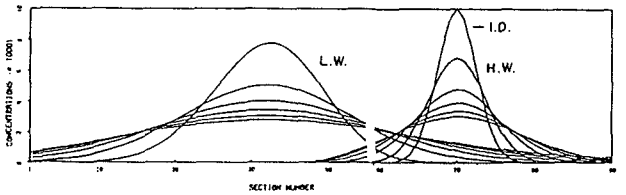

Figure 6.

The test described under 3.2 was repeated for a channel in which a portion of the channel was split up into several branches as shown in Figure 4. Figure 5 shows the results from a computation with only advective transport; for those in Figure 6 dispersive transport was also taken into account. The numerical dispersion (Figure 5) is slightly more than in the previous test (Figure 2) but still very small when compared with the simulation in which dispersive transport was included (Figure 6).

3.4 Channel with Constriction

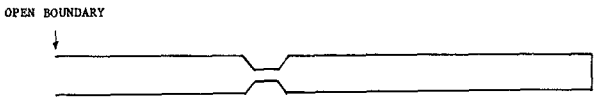

Figure 7.

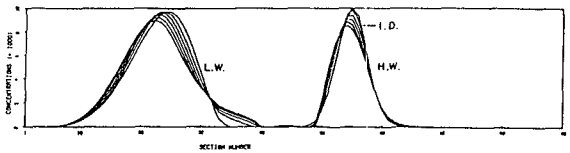

Figure 8.

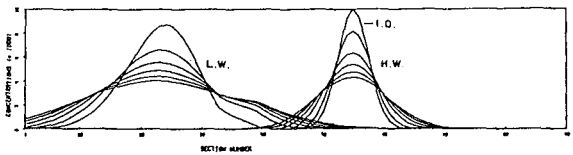

Figure 9.

The same test (3.2) as repeated for a channel with a constriction in it (Figure 7). Again the numerical dispersion with only advective transport (Figure 8) is very small compared to the model test in which dispersive transport was also taken into account (Figure 9).

4. APPLICATION TO KNYSNA ESTUARY

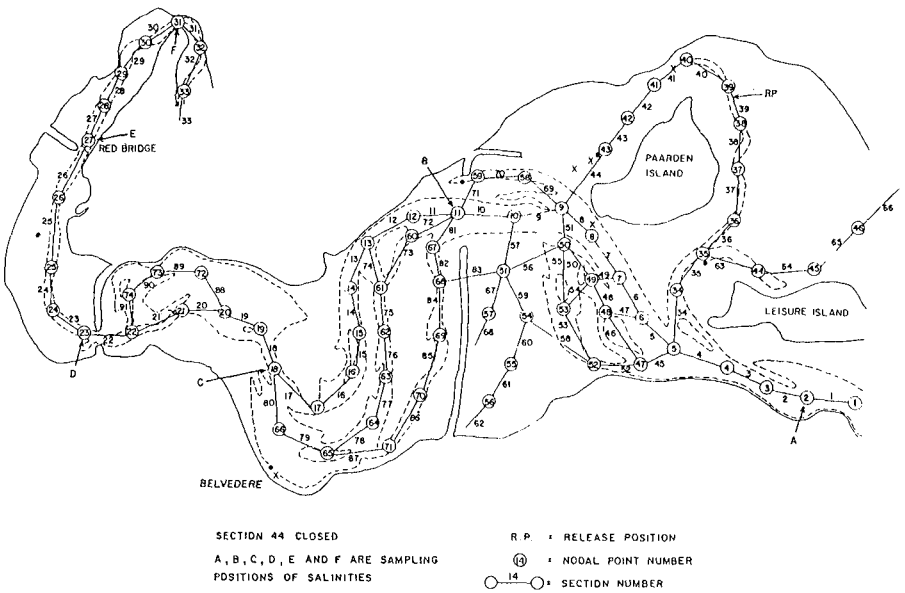

Figure 10.

4.1 General

The Knysna estuary on the south coast of South Africa has a complicated channel system, with extensive flood plains in the downstream area (Figure 10). At the upstream end fresh water from the Knysna river enters the estuary causing gradients in salinity concentrations along

the estuary. Increasing demands for fresh water have led to investigations of the feasibility of extracting water from the Knysna river upstream of the estuary. The problem is to determine the effect this could have on the salinity distributions and variations and on the ecology of the estuary. Salinity concentrations were measured on a certain day, then the river flow was monitored and after a period of about seven days the salinities were measured again. An estimation was made for the dispersion coefficients in the estuary. With these data available, model simulations were done. The starting conditions were the salinity distributions of the beginning of a period. At the open sea boundary a recorded tidal variation was used and at the upstream end the recorded river flow was used for boundary conditions. The salinities computed with the model after the period were then compared with the measured salinities of the corresponding time. A reassesment was then made of the dispersion coefficients and the model simulation was repeated. After a few tests good agreement was achieved between model results and prototype data and the model was considered to be calibrated. Verification runs were done for other periods with equally good results. A number of model tests were then done under different flow conditions for investigating salinity distributions under these circumstances.

4.2 Calibration Tests

In Figure 11A the start condition is shown, which was measured at low water on 18 January 1984 and which was used for the calibration runs. The period covered by the tests was from 18 till 25 January 1984. The river flow was constant at 0,8 m^3/s and at the open sea boundary the water level variation was recorded. A first estimation of the dispersion coefficient (K) was made using formula 2.8. In the first calibration test K = 45 m^2/s was used for all the sections. The model results are compared on Figure 11B for 25 January 1984. The model results are slightly higher compared to the field data in the upstream region (Sections 23 to 33) of the estuary.

A second calibration test was done in which K = 45 for all sections except K = 35 for Sections 23 to 26 and K = 25 for Sections 27 to 32. The model results are now slightly too low at the upstream region of the estuary indicating that the adaptation was a little too drastic (Figure 11C).

A third calibration test was therefore done in which K = 45 for all sections except K = 40 for Sections 23 to 26 and K = 35 for Sections 27 to 32. Figure 11D shows that excellent agreement between model results and field data was achieved. In all further tests these dispersion coefficients were used.

4.3 Verification Tests

The first verification test was done for the period 10 to 17 March 1984. The flow was variable from 1,82 m^3/s on 10/03/1984 to 2,90 m^3/s on 13/03/1984 to 1,15 m^3/s on 17/03/1984. The agreement between model results and prototype data was still good for 17/03/1984, although the river flow data was probably not very accurate (Figure 12B).

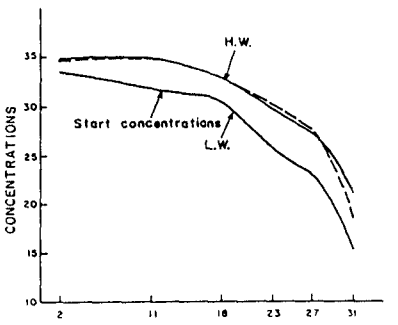

A. Simulation 1
Date: 18.1.1984
Start conditions at L.W.
K = 45.00 for all sections
Flow = 0.8 m^3/s.

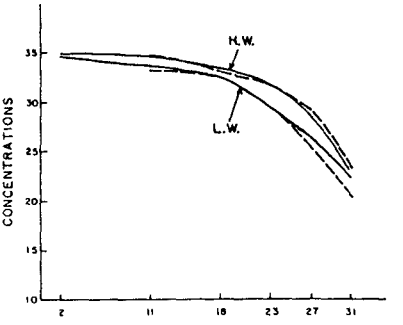

B. Simulation 1
Date: 25.1.1984
K = 45.00 for all sections
Flow = 0.8 m^3/s.

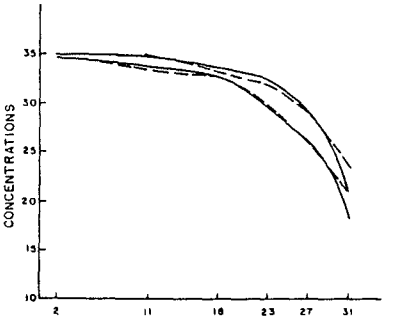

C. Simulation 2
Date: 25.1.1984
K = 45.00 sections 1-22, 33-74
K = 35.00 Sections 23-26
K = 25.00 Sections 27-32
Flow = 0.8 m^3/s.

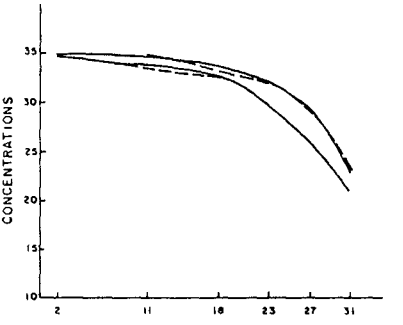

D. Simulation 3
Date: 25.1.1984
K = 45.00 Sections 1-22, 33-74
K = 40.00 Sections 23-26
K = 35.00 Sections 27-32
Flow = 0.8 m^3/s.

——= computed concentrations
----= field measurements

Figure 11

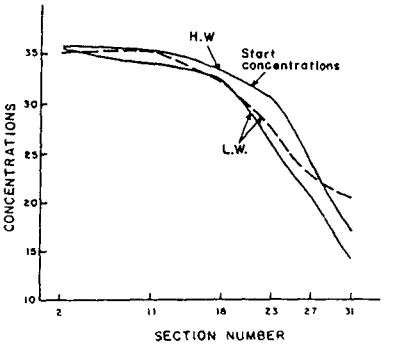

A. Simulation 4
Date: 10.3.1984
Start conditions at H.W.
K = 45.00 Sections 1-22, 33-74
K = 40.00 Sections 23-26
K = 35.00 Sections 27-32

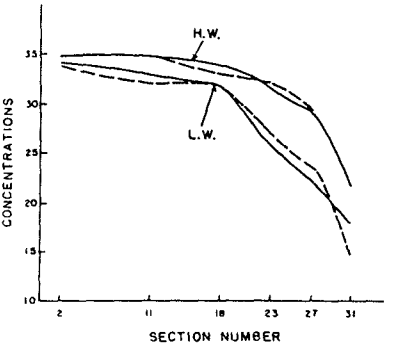

B. Simulation 4
Date: 17.3.1984
Flow: Variable

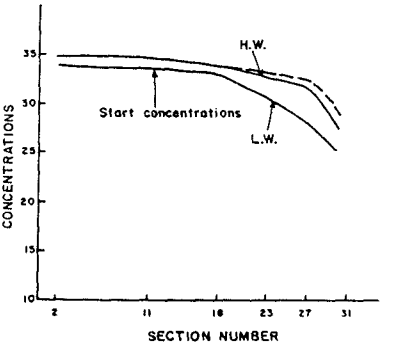

C. Simulation 5
Date: 16.4.1984
K = same as simulation 4
Flow: variable.

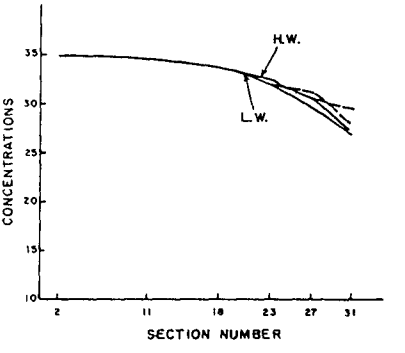

D. Simulation 5
Date: 23.4.1984
K = same as simulation 4
Flow: variable.

——— = computed concentrations
– – – – = field measurements

Figure 12

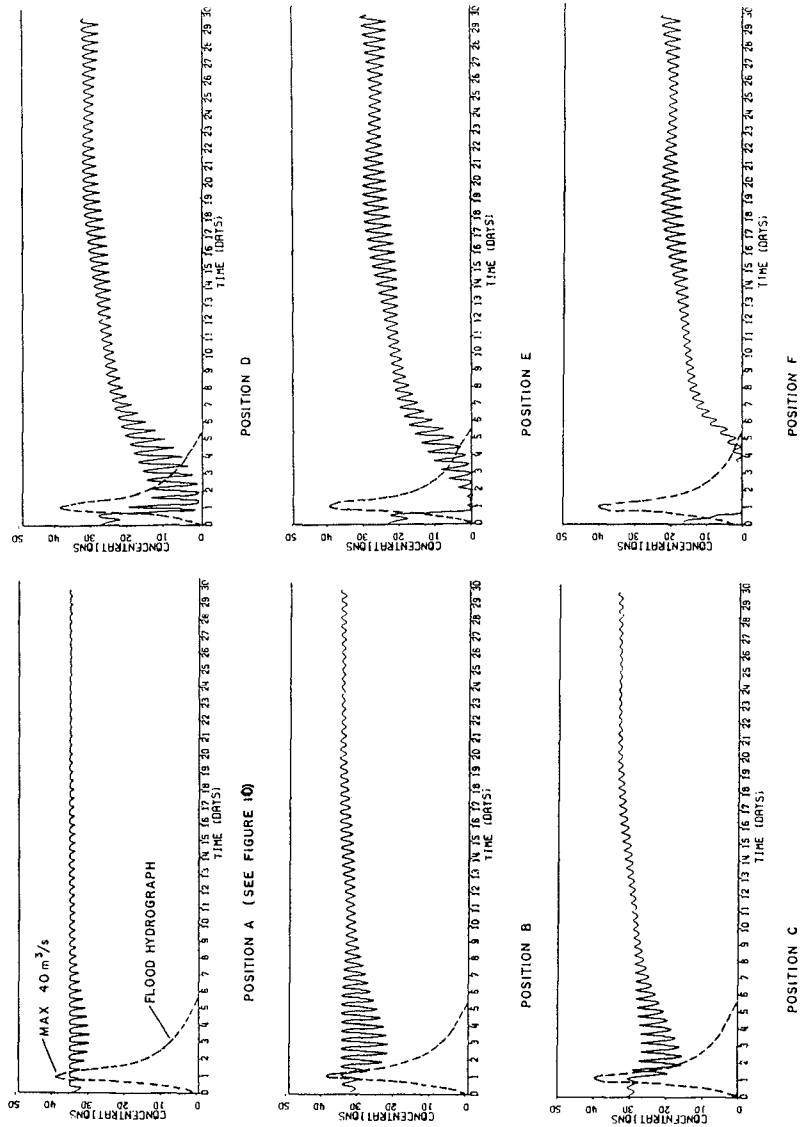
MAX 40 m³/s
FLOOD HYDROGRAPH
CONCENTRATIONS
TIME (DAYS)
POSITION A (SEE FIGURE 10)
POSITION B
POSITION C
POSITION D
POSITION E
POSITION F

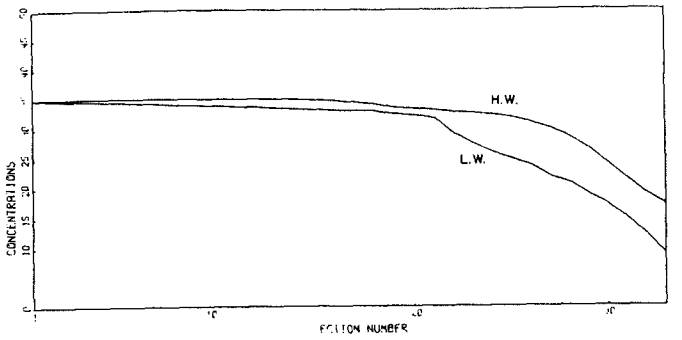

A. SALINITIES AT SPRINGTIDE AND RIVER FLOW OF 1.0 m^3/s

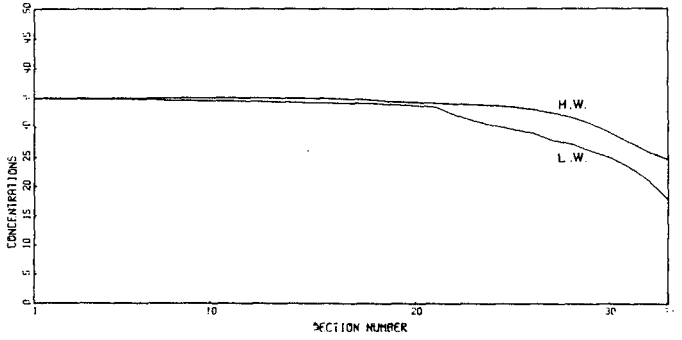

B. SALINITIES AT SPRINGTIDE AND RIVER FLOW OF 0.5 m^3/s

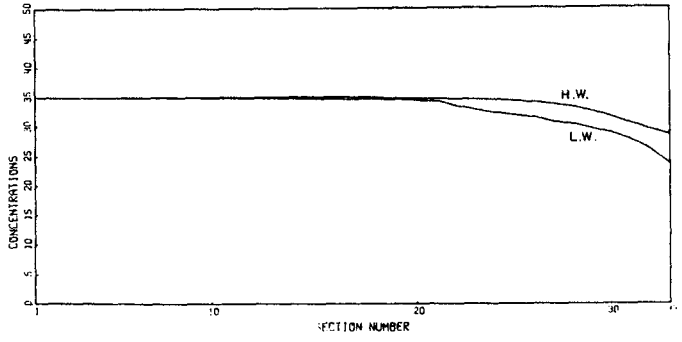

C. SALINITIES AT SPRINGTIDE AND RIVER FLOW OF 0.3 m^3/s

Figure 14

A second verification test was done for the period 16 to 23 April 1984. The flow data used was 0,85 m^3/s for 16 to 19/04/1984, 0,70 m^3/s for 20 and 21 April 1984 and 0,60 m^3/s for 22 and 23 April 1984. The results again show good agreement between model and prototype results (Figure 12D).

4.4 River Flood Test

On Figure 13 the effects of a minor river flood on the salinities in the estuary is shown. The shape of the hydrograph with a maximum flow of 40 m^3/s is shown on each graph.

At the upstream end of the estuary, positions E and F (see also Figure 10), the salinities drop down to zero but later return to their normal values. The graphs for positions A, B, C and D all show the effects of this flood, with the strongest influence upstream in the estuary and the weakest effect near the estuary mouth. On all the graphs the effect of the spring-neap-spring tidal variation is also visible.

4.5 Tests under different constant-flow conditions (1,0, 0,5 and 0,3 m^3/s)

The start condition in all these tests was the salinity distributions as measured at low water on 18 January 1984. The results are shown as graphs of distributions in the main channel of the estuary in Figure 14.

For Sections 1 to 22 all the graphs show little difference between high and low water, but considerably bigger differences for Sections 23 to 33, in the narrow upper channel of the estuary. It can also be seen that the influence of the fresh water inflow is considerable at the upper end of the estuary, but small in the downstream part (Sections 1 to 22).

4.6 Details of Computation

The Knysna model tests were done at a timestep of 30 seconds to fulfil the Courant criterion for the hydrodynamic computation (formula 2-12). As stated before (Section 2.5) the hydrodynamic and water quality computations were done at the same timestep. The operation of the Knysna model on the CDC-cyber 750 computer could be done at a cost of about $10 a day (prototype time).

5. CONCLUSIONS

The model presented is one-dimensional and is also 100 per cent conservative. Simulations with test models of simple geometrical structure show that the numerical dispersion is very small. This numerical dispersion increases slightly at models with irregular topography and networks, but for the test cases described here this dispersion was always very small.

As shown by its application to the Knysna estuary, the model is easily applicable to suitable estuaries, which means estuaries that are

vertically well-mixed and in which two-dimensional horizontal current patterns are negligible.

The calibration and verification runs for the Knysna estuary in particular show the reliability of the model and the subsequent tests for different flow conditions show the potential of the model as a tool for investigations of the influences of these conditions on salinities and these results can be used for further ecological studies.

The model could be developed further to simulate chemical and biological processes, but it would probably be better to use the other existing models, like the Dynamic Estuary Model (DEM) from the Environmental Protection Agency (EPA) in the USA. As mentioned before, the model presented here has similar features to this DEM.

Finally, the present combination of the hydro-dynamical with the water-quality model computations has the disadvantage that the model has to be operated on a small section length (100 to 500 m) and time-step (30 to 60 seconds). It was possible though to carry out the tests at relatively low cost. The Knysna model for example, was operated at about $10 per day or $300 per month. This shows that the model can be a practical tool for many investigations at reasonable cost.

LIST OF SYMBOLS

ATR = advective transport

A_x, A_N = cross-sectional area at x or N (m^2)

C = concentration (kg/m^3)

C_N = concentration of position N (kg/m^3)

Cf = Chezy coefficient ($m^1/^2/s$)

CTR = sum of all advective and diffusive transport to and from a nodal position

Df = constant used which is actually Df = $Df^1.\sqrt{2g}$ in formula for diffusion coefficient (2-7)

DTR = diffusive transport

DW = diffusion coefficient (m^2/s)

dx_N, dx_M = nodal length at N, section length at M (m)

K = dispersion coefficient (m^2/s)

M = identification of section number (also as subscript)

N = identification of nodal number (also as subscript)

Q, Q_M = flow through cross-section (M) (m^3/s)

R = hydraulic radius (m)

S = salinity concentration (mg/ℓ)

t = time (s)

Δt = timestep of computation (s)

u_M = mean velocity (m/s)

u_N = net downstream velocity due to fresh water discharge

Vol = volume (m^3)

x = distance (m)

^{1} = all variables marked like this are on a new time level

LIST OF REFERENCES

CSIR (1976). Saldanha Bay, the assessment of field data, the mathematical model and the physical model, Volume II. CSIR Report C/SEA 7620/2.

FISHER, H B, LIST, E J, KOH, R C Y, IMBERGER, J and BROOKS, N H (1979). Mixing in inland and coastal waters. New York.

LEENDERTSE, J J (1970). A water-quality simulation model for well-mixed estuaries and coastal seas. Volume I, principles of computation. RM-6230-RC.

ORLOB, G T (1972). Mathematical modelling of estuarial systems. International symposium on modelling techniques in water resources systems. Ottawa.